Acta Crystallographica Section B
Structural Science
ISSN 0108-7681

On the structure of aragonite – Lawrence Bragg revisited

D. J. M. Bevan,[a]* Elisabeth Rossmanith,[b] Darren K. Mylrea,[c] Sharon E. Ness,[c] Max R. Taylor[a] and Chris Cuff[c]

[a]School of Chemistry, Physics and Earth Sciences, The Flinders University of South Australia, GPO Box 2100, Adelaide SA 5001, Australia, [b]Mineralogisches Institut, University of Hamburg, Grindelallae 48, D-20146 Hamburg, Germany, and [c]Advanced Analytical Centre, James Cook University, Townsville, Queensland, Australia

Correspondence e-mail: judge.bevan@flinders.edu.au

Received 22 October 2001
Accepted 18 February 2002

The structure of aragonite was first determined by Lawrence Bragg in 1924 in what is the now standard space-group setting *Pnma* (No. 62). Subsequent studies have all taken his structure as their starting points, despite Bragg's own stated doubts and some earlier etching studies which indicated that the underlying symmetry may really be polar. We have reinvestigated the structure and found that there are many reflections with significant intensity among those that should be systematically extinct in *Pnma*. Some of these reflections have been subjected to further experimental analysis and have been shown not to be due to Renninger effects. A possible model that satisfies these observations is one where the true structure is in space group $P\bar{1}$ and the structure is twinned about the three axial twofold rotation axes of *Pnma*. The space group *P*1 cannot be ruled out. Evidence for these conclusions is presented. The crystal chemistry of aragonite is revisited and described in terms of the stuffed alloy CaC. The carbonate group is confirmed to be non-planar in the crystal.

1. Introduction

Calcium carbonate is a compound that commonly exhibits polymorphic variation. The orthorhombic form, aragonite, played an important role in the discovery of polymorphism by Mitscherlich in 1822 (Mitscherlich, 1822) and of isomorphism by Wollaston in 1812 (Wollaston, 1812). Although usually considered to be a high-pressure polymorph, aragonite is commonly precipitated biogenically and metastably in marine environments by invertebrates as diverse as scleractinian corals and giant clams (Tridacnids).

Crystal structure and chemistry are integral to any understanding of polymorphs in terms of stability and reactivity. The arrangement of atoms in a crystal structure and the constraints imposed by coordination and bonding also exert a profound influence on crystal growth. Similarly, differences in structure and bonding, and consequently of physical properties, control stability differences between polymorphs. These interrelationships are especially germane to the present considerable interest in the geochemistry of aragonite, especially insofar as trace-element (Sr, Ba, Pb, Mn and Cd) content and isotope ratios ($^{18}O/^{16}O$, $^{13}C/^{12}C$ and $^{14}C/^{12}C$) can be used as environmental indicators. As a consequence, it has become essential to understand more fully the structural factors which might influence the uptake of trace elements and isotopic distributions. This is particularly true for the isotopic ratios, where partitioning is a function of the thermal lattice vibrations (Broeker & Oversby, 1971) which, in turn, relate to the crystal structure.

Table 1
Sample analyses (p.p.m. by weight).

Ca × 10^5	Mg	Na	Fe	Sr	K	Cr	Pb	Cd	Mn	Cu	Zn
3.905	19	67	719	6968	16	70	240	23	108	31	†
3.966	6	44	607	5125	11	71	268	27	93	27	†

† 'Below the detection limit' for that element.

This structure was first determined by Lawrence Bragg in 1924 (Bragg, 1924). His work was indeed a *tour de force* at the time, because it was the first structure determination involving more than one variable parameter: nine were determined and for the first time Bragg discussed crystal symmetry in terms of formal space-group theory (Phillips, 1979). The now standard space-group setting is *Pnma* (No. 62). Moreover, his stature was such that subsequent refinements (de Villiers, 1971; Dickens & Bowen, 1971; Dal Negro & Ungaretti, 1971; Jarosch & Heger, 1986) have all taken his structure as their starting points, despite Bragg's own stated doubts: '*The analysis which is described below places aragonite in the holosymmetric class of the orthorhombic system, and* ***though it is always possible that the actual structure may have a lower symmetry owing to some distortion which is not revealed by X-ray examination, it would appear that this distortion is very small*** *(our emphasis)*'. Indeed, Bragg also refers to earlier etching studies which '*..indicate that the symmetry may really be polar*'.

Some time ago, studies on a variety of aragonites from Abu Dhabi (Cuff, 1969), using both single-crystal and powder X-ray diffraction techniques, revealed splitting of normally coincident reflections, together with the occurrence of weak reflections that violated the *Pnma* space-group conditions. More recently, Belda *et al.* (1993) and Rasmussen *et al.* (1992) found consistent splitting in three reflections from Tridacna gigas and Porites *sp.* corals, which seemed to correlate well with environmental parameters off the Australian North Queensland coast. Also, Mylrea (1991) has observed line splitting in Hägg–Guinier powder diffraction patterns from a mineral sample.

In a different context, extensive theoretical research has been carried out by Catti *et al.* (1993) to model thermodynamic, energetic, structural and elastic properties of calcite and aragonite. This has been done successfully for calcite, but aragonite has proved rather intractable. This correlates with major problems in the interpretation of the IR and Raman spectra of the mineral aragonite. White (1974), Frech *et al.* (1980) and Gillet *et al.* (1993) have pointed out inconsistencies (band-splitting, for example) between the observed vibrational spectra and what would be expected from normal mode assignments assuming *Pnma* symmetry, and Kraft *et al.* (1991) have also emphasized the complexity of the spectroscopic data for aragonite and the lack of agreement between researchers on mode assignments. A possible cause, suggested by several authors (Adler & Kerr, 1963; Scheetz & White, 1970), is lower site symmetry for the carbonate group.

Taken together, all these factors have led us to undertake a careful reassessment of Bragg's structure for aragonite.

2. Experimental

Programs from the *Xtal*3.4 system (Hall *et al.*, 1995) were used for all conventional crystallographic calculations.

2.1. Sample selection and data collection

After careful searching, a mineral crystal was chosen from a sample of unknown origin obtained from the British Museum, the same sample from which line-splitting in Guinier–Hägg powder diffraction experiments had been observed (Mylrea, 1991). Duplicate analyses of this sample by atomic absorption spectrophotometry are shown in Table 1. The major impurity is Sr at *ca* 1 atom%.

The crystal shape approximated that of a hexagonal prism. Optical examination and Buerger precession photographs showed that it was untwinned macroscopically. This crystal was then transferred to a CAD-4 diffractometer, and its diffraction properties were explored using Mo $K\alpha$ radiation (λ = 0.7107 Å) with φ–2θ scans. This one crystal has been explored in one way or another on four different CAD-4 diffractometers and the refined cell parameters obtained in these four independent experiments illustrate the well known discrepancies between data obtained from different instruments. Nevertheless, we would have to conclude that the cell is metrically orthorhombic. The unit-cell dimensions used in this study, along with other crystal data, are given in Table 2.[1]

Initially, a half-sphere of data was collected in the normal manner (φ = 0) and evaluated: some reflections ($0kl$; $k + l = 2n + 1$: $hk0$; $h = 2n + 1$), forbidden in the *Pnma* space group, although weak, seemed to be present and a full sphere of data was then collected. However, in these two data collections, too many of the weak reflections were flagged as such in the fast preliminary scan and were therefore not measured. In a second experiment on the same crystal, another whole sphere of data was collected on another CAD-4 diffractometer, from which the unit-cell dimensions in Table 2 were obtained, this time ensuring that every reflection was measured for 45 s, with *psi* again at zero. This is the data set used in this study.

2.2. Data assessment

The full data set ($0 < \theta < 40^\circ$) contained 2794 reflections for which the Friedel pairs had been averaged. Of these, 168 were 'forbidden' in *Pnma* and of these 168 reflections there were 74 for which I_{obs} was greater than $2\sigma I_{obs}$. Moreover, this set contained 23 reflections for which I_{obs} was greater than $5\sigma I_{obs}$ and 9 for which I_{obs} was greater than $10\sigma I_{obs}$. These intensities cannot be ignored, although the I_{obs} values are of the order of one thousandth of those of the strong reflections. In addition, this group contains some $h00$, $0k0$ and $00l$ reflections for which h, k and l, respectively, are odd, thus potentially precluding a,

[1] Supplementary data for this paper are available from the IUCr electronic archives (Reference: BR0111). Services for accessing these data are described at the back of the journal.

b and *c* as 2_1 axes. The issue now is to determine whether or not these 'forbidden' reflections are genuinely present, thus demanding a lowering of the crystal symmetry from *Pnma*, or appear as a result of double diffraction, a phenomenon well known in electron diffraction but largely ignored by X-ray

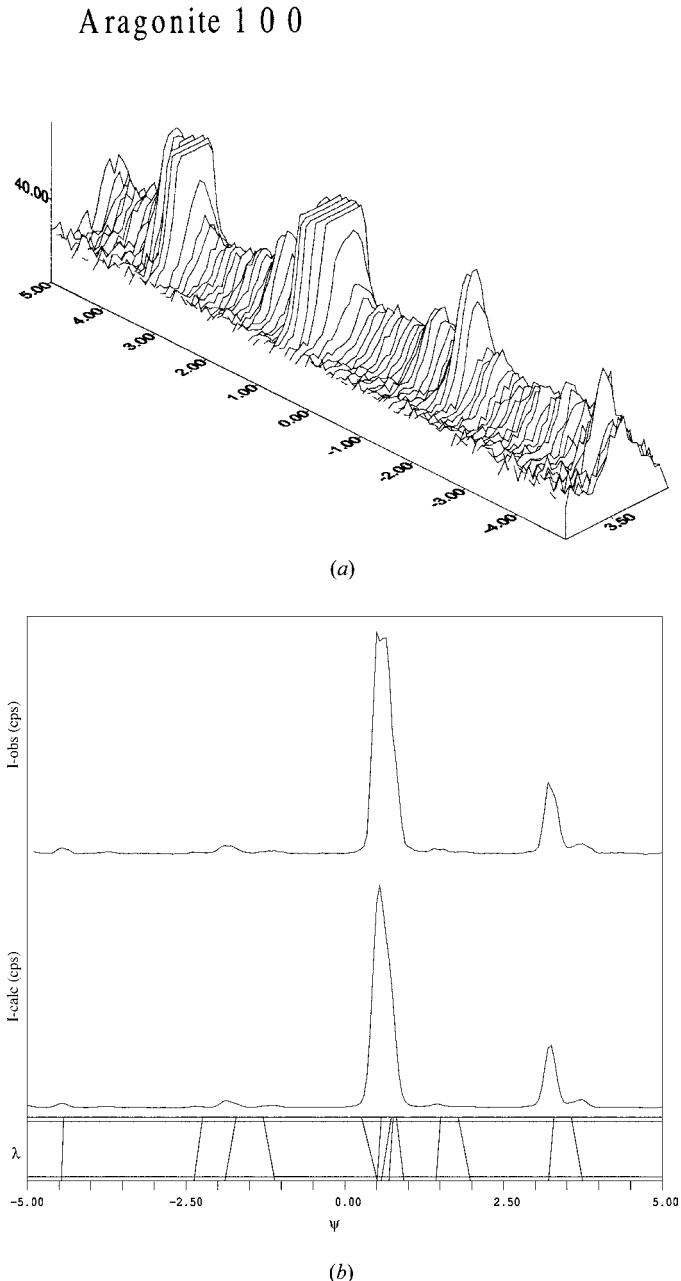

Figure 1
Intensity profile representation for 100 reflections. (*a*) The three-dimensional representation depicts an intensity profile over a small ω range as a function of ψ. The large double diffraction spikes have been truncated. The 'observed intensity' for the reflection is the mean value of the ω-integrated intensities measured in a range of ψ where no double diffraction events are calculated. (*b*) The observed and calculated intensities as a function of ψ. The bottom panel shows the double diffraction events with $I_{cps} \geq 0.10$ plotted in the $\psi - \lambda$ diagram. The following parameters were used in the calculations: wavelength: Mo $K\alpha_{1,2}$; divergence of the incident beam: 0.14°; radius of the sample: 200 μm; mosaic spread of the sample: 0.015°; mosaic block radius: 0.4 μm.

Table 2
Experimental details.

Crystal data	
Chemical formula	$CaCO_3$
Chemical formula weight	100.08
Cell setting, space group	Triclinic, $P\overline{1}$
a, b, c (Å)	5.7394 (4), 4.9616 (2), 7.9700 (5)
α, β, γ (°)	90.004 (4), 90.012 (5), 90.001 (4)
V (Å^3)	226.96 (2)
Z	4
D_x (Mg m^{-3})	2.929
Radiation type	Mo $K\alpha$
No. of reflections for cell parameters	25
θ range (°)	22.4–39.1
μ (mm^{-1})	2.468
Temperature (K)	293
Crystal form, colour	Hexagonal prism, colourless
Crystal size (mm)	0.54 × 0.15 × 0.13
Data collection	
Diffractometer	CAD-4
Data collection method	$\theta/2\theta$ scans
Absorption correction	Gaussian
T_{min}	0.675
T_{max}	0.730
No. of measured, independent and observed parameters	5690, 2794, 2750
Criterion for observed reflections	$F^2 > 0$
R_{int}	0.02
θ_{max} (°)	39.92
Range of h, k, l	$-10 \rightarrow h \rightarrow 10$ $-8 \rightarrow k \rightarrow 8$ $-14 \rightarrow l \rightarrow 14$
No. and frequency of standard reflections	3 every 120 min
Refinement	
Refinement on	F^2
$R[F^2>2\sigma(F^2)]$, $wR(F^2)$, S	0.026, 0.056, 1.81
No. of reflections and parameters used in refinement	2750, 32
Weighting scheme	$w = 1/[\sigma^2(F_o^2) + (0.04F_o^2)^2]^{1/2}$
$(\Delta/\sigma)_{max}$	0.0007
$\Delta\rho_{max}$, $\Delta\rho_{min}$ (e Å^{-3})	2.14, −1.89
Extinction method	Becker & Coppens (1975)
Extinction coefficient	867 (62)

crystallographers since it was first reported by Renninger (1937). It has been studied in great detail more recently by Rossmanith (1992, 1999). In essence, what occurs in double diffraction is that a strong primary diffraction beam can act as the incident beam for further diffraction and thus give rise to these 'forbidden' reflections (Arndt & Willis, 1966). Fortunately, however, in four-circle diffractometry, the mounted crystal can be rotated about the diffraction vector for any given reflection, so that the Bragg condition is fulfilled at all times, the rotation angle being *psi*, and intensities can be measured many times at different *psi* values: this constitutes a *psi* scan, from which the true presence or absence of the reflection scanned can be inferred.

One of us (ER) has carried out experiments which demonstrate very clearly that some reports of symmetry lowering, based on the observation of 'forbidden' reflections, are suspect because these reflections can be attributed to double diffraction (Rossmanith & Armbruster, 1995). This work used very careful exploration of *psi* scans at very small

intervals over a considerable angular range. These were then compared with the double-diffraction profiles for the 'forbidden' reflections, computed with the program *UMWEG*98 (based on theory developed by Rossmanith, 1992, 1999: the agreement was excellent. We have adopted this approach, therefore, in order to resolve the problem with aragonite.

In a third experiment, 29 of the stronger 'forbidden' reflections in *Pnma* were explored. *Psi* scans were made over a total angular range of 4° at intervals of 0.1°: the count time for each data point was 6 min. The resulting 40 integrated intensities for each reflection were then assessed: double diffraction effects were apparent in most cases. From these data, it was possible to choose 7 reflections which appeared to have significant intensity at all points of the *psi* scan, with any double diffraction effects superimposed on this base. In a fourth experiment, these were then subjected to more detailed *psi* scans in which the angular range of *psi* was increased to 10° and the intervals decreased to 0.05°. The results have been analysed with the program *UMWEG*98 and it can be stated quite categorically that the measured reflections 010, 110 and 003 are truly present, with a high probability that 100 is also present. The results of this analysis are presented in Figs. 1–4. For the other three (001, 012 and 120), it is not possible to conclude one way or the other.

Single-crystal neutron diffraction data from a different crystal, measured at the Australian National Scientific and Technology Organization (ANSTO) with a neutron wavelength of 1.2330 Å, add further support to this conclusion. These data also indicate the presence of 010, 100, 110, 003 and,

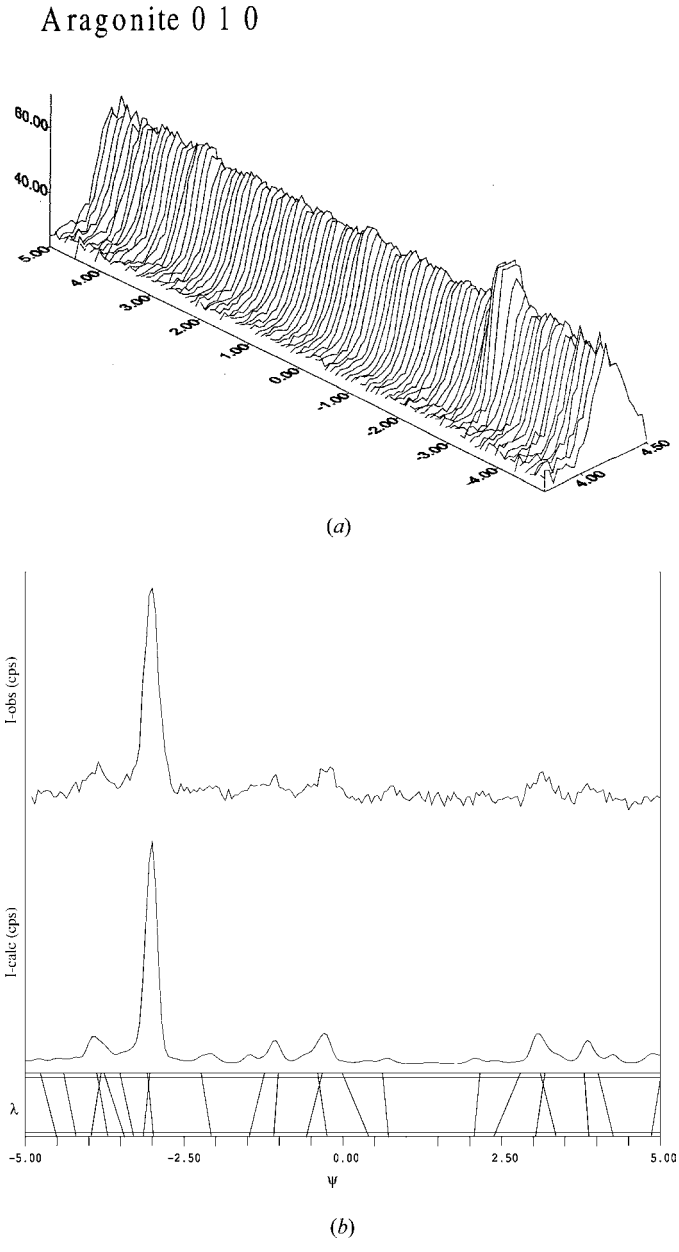

(*a*)

(*b*)

Figure 2
Intensity profile representation for 010 reflections. (*a*) and (*b*) as in Fig. 1.

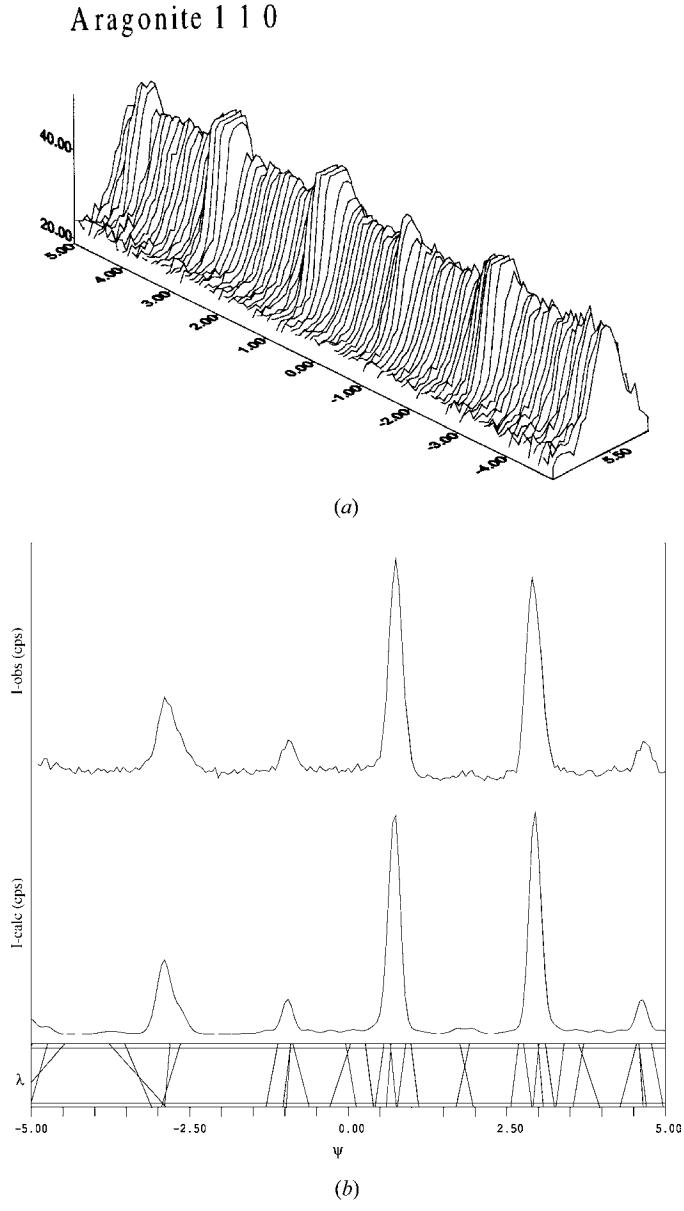

(*a*)

(*b*)

Figure 3
Intensity profile representation for 110 reflections. (*a*) and (*b*) as in Fig. 1.

additionally, 030, 050, 300, 500, 700 (as do the X-ray data; see below), although no significant neutron intensity was recorded for 012 and 120. However, they have not been subjected to UMWEG98 analysis for double diffraction. Nevertheless, the evidence is convincing for the genuine occurrence of reflections from aragonite which are forbidden in the *Pnma* space group. This result has the effect of reducing the symmetry of **our** aragonite crystal at least to $P\bar{1}$, since the extinction conditions for the symmetry elements of space group *Pnma* and its orthorhombic or monoclinic subgroups no longer exist. The possibility that the true symmetry may even be *P*1 is indicated by Bragg's (1924) reference (see above) to etching experiments, suggesting a polar structure.

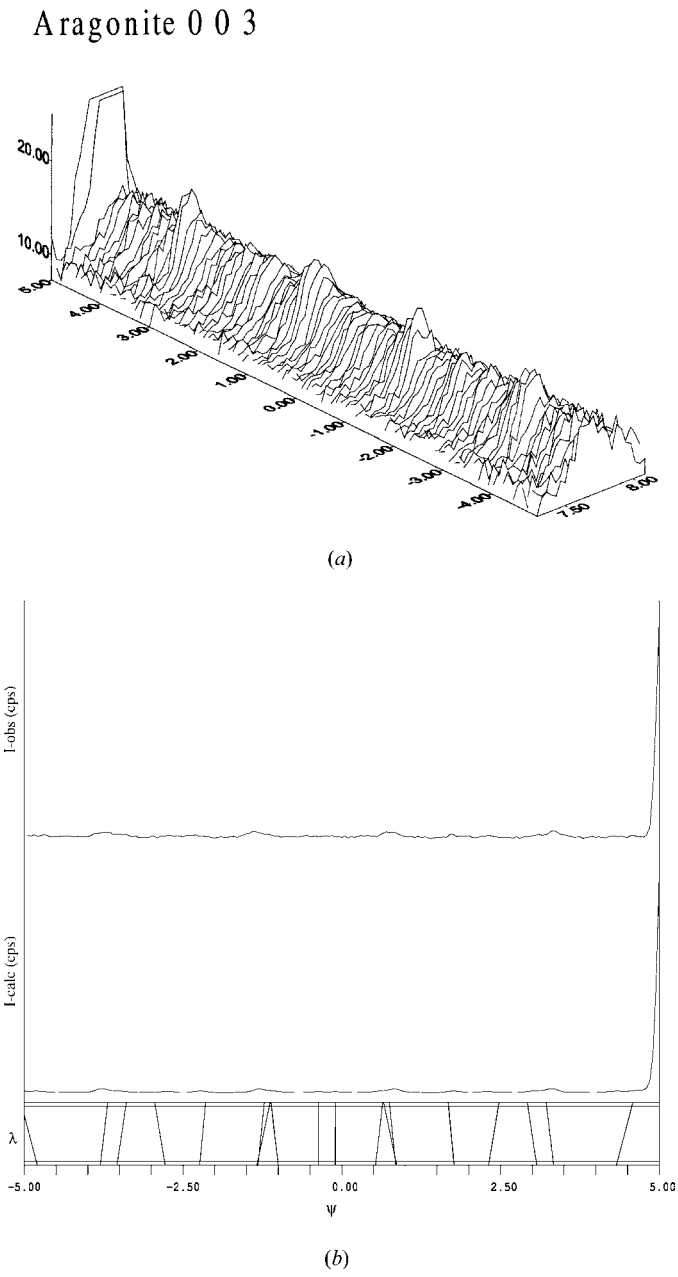

Figure 4
Intensity profile representation for 003 reflections. (*a*) and (*b*) as in Fig. 1.

Attempts to gain further relevant information using convergent-beam electron diffraction yielded inconclusive results, not least because of the extreme sensitivity of aragonite samples in the beam.

3. The structure of aragonite

The X-ray intensity data from the experiment in which all reflections were measured for 45 s were used to explore the structure. Atom positions initially were taken from the

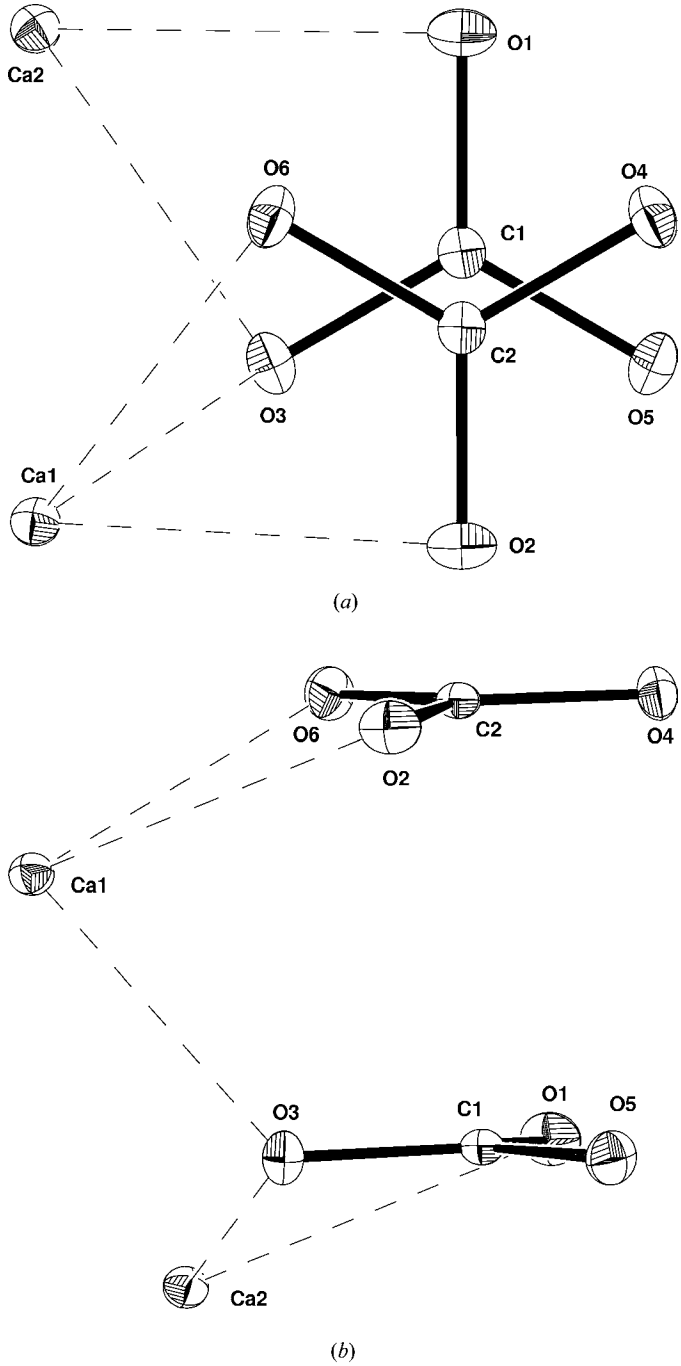

Figure 5
Two views of the displacement ellipsoids obtained in refinement **R1** and used in **R5** at the 50% probability level.

Table 3
Observed and calculated values of $|F|$ for 'forbidden' reflections.

R1–**R5** are defined in the text.

h	k	l	F_{obs}	**R1** F_{calc}	**R2** F_{calc}	**R3** F_{calc}	**R4** F_{calc}	**R5** F_{calc}
0	0	1	**0.30**	0.02	0.18	0.31	**0.08**	**0.20**
0	0	3	**0.87**	0.03	0.54	0.18	**0.78**	**0.87**
0	0	5	**0.55**	0.04	0.50	0.44	**0.44**	**0.40**
0	1	−12	**0.94**	0.03	0.27	0.79	**0.41**	**0.40**
0	1	−6	**0.40**	0.02	0.57	0.51	**0.52**	**0.51**
0	1	−4	**0.34**	0.02	0.39	0.51	**0.47**	**0.44**
0	1	−2	**0.48**	0.01	0.43	0.49	**0.38**	**0.44**
0	1	0	**1.17**	0.05	0.67	0.63	**0.55**	**0.54**
0	1	2	**0.38**	0.01	0.43	0.49	**0.38**	**0.44**
0	1	6	**0.54**	0.07	0.57	0.51	**0.52**	**0.51**
0	1	10	**0.63**	0.01	0.33	0.25	**0.43**	**0.36**
0	1	12	**0.76**	0.06	0.27	0.79	**0.41**	**0.40**
0	2	−13	**0.64**	0.02	0.14	0.09	**0.35**	**0.33**
0	2	−5	**0.46**	0.01	0.52	0.76	**0.33**	**0.34**
0	2	−3	**0.48**	0.03	0.52	0.61	**0.55**	**0.57**
0	2	1	**0.39**	0.02	0.38	0.36	**0.30**	**0.30**
0	2	3	**0.52**	0.08	0.52	0.61	**0.55**	**0.57**
0	2	5	**0.67**	0.02	0.52	0.76	**0.33**	**0.34**
0	3	−10	**0.51**	0.04	0.61	0.21	**0.25**	**0.22**
0	3	−8	**0.54**	0.01	0.49	0.53	**0.27**	**0.38**
0	3	−6	**0.50**	0.01	0.45	0.71	**0.56**	**0.61**
0	3	−4	**0.55**	0.01	0.39	0.33	**0.40**	**0.39**
0	3	0	**0.43**	0.06	0.52	0.64	**0.51**	**0.52**
0	3	2	**0.38**	0.02	0.43	0.54	**0.42**	**0.47**
0	3	10	**0.81**	0.01	0.62	0.21	**0.25**	**0.22**
0	4	−9	**0.68**	0.03	0.54	0.56	**0.54**	**0.53**
0	4	3	**0.46**	0.08	0.37	0.72	**0.41**	**0.37**
0	4	5	**0.45**	0.05	0.25	0.53	**0.32**	**0.32**
0	4	9	**0.62**	0.06	0.54	0.56	**0.54**	**0.53**
0	5	−4	**0.64**	0.02	0.51	0.11	**0.10**	**0.22**
0	5	0	**1.11**	0.08	1.16	0.98	**1.12**	**1.11**
0	5	2	**0.50**	0.09	0.43	0.20	**0.32**	**0.36**
0	6	−9	**0.89**	0.01	0.26	0.75	**0.47**	**0.47**
0	6	−7	**0.74**	0.08	0.40	0.16	**0.26**	**0.22**
0	6	9	**1.03**	0.07	0.26	0.75	**0.47**	**0.47**
0	8	−5	**1.07**	0.02	0.50	0.57	**0.18**	**0.21**
1	−6	0	**0.50**	0.07	0.85	0.86	**0.80**	**0.86**
1	−3	0	**0.66**	0.02	0.63	1.13	**0.78**	**1.13**
1	−2	0	**1.64**	0.04	0.77	0.95	**0.82**	**0.95**
1	−1	0	**1.15**	0.01	0.46	0.55	**0.59**	**0.55**
1	0	0	**0.91**	0.00	0.29	0.21	**0.27**	**0.21**
1	1	0	**1.12**	0.02	0.47	0.55	**0.59**	**0.55**
1	2	0	**1.61**	0.00	0.76	0.95	**0.82**	**0.95**
1	3	0	**0.78**	0.02	0.61	1.13	**0.78**	**1.13**
3	−8	0	**0.70**	0.00	0.55	0.27	**0.33**	**0.27**
3	−6	0	**1.00**	0.05	0.73	0.89	**0.64**	**0.89**
3	−5	0	**1.38**	0.03	0.94	0.70	**0.31**	**0.70**
3	−4	0	**0.56**	0.00	0.53	0.69	**0.43**	**0.69**
3	−2	0	**0.82**	0.02	0.80	1.03	**0.83**	**1.03**
3	−1	0	**0.54**	0.03	0.56	0.70	**0.66**	**0.70**
3	0	0	**0.75**	0.01	0.76	0.86	**0.67**	**0.86**
3	1	0	**0.55**	0.04	0.55	0.69	**0.66**	**0.69**
3	2	0	**0.68**	0.02	0.84	1.04	**0.83**	**1.04**
3	5	0	**1.12**	0.01	0.91	0.69	**0.31**	**0.69**
3	6	0	**0.98**	0.01	0.75	0.90	**0.64**	**0.90**
3	8	0	**0.96**	0.01	0.57	0.27	**0.33**	**0.27**
5	−6	0	**0.99**	0.00	0.58	0.77	**0.76**	**0.77**
5	−2	0	**0.43**	0.02	0.23	0.76	**0.65**	**0.76**
5	−1	0	**0.43**	0.01	0.62	0.58	**0.25**	**0.58**
5	0	0	**0.55**	0.02	0.54	0.08	**0.61**	**0.08**
5	1	0	**0.53**	0.01	0.61	0.58	**0.25**	**0.58**
5	3	0	**0.50**	0.01	0.52	0.43	**0.68**	**0.43**
5	6	0	**1.06**	0.08	0.56	0.77	**0.76**	**0.77**
7	−6	0	**0.92**	0.02	0.71	0.81	**0.61**	**0.81**
7	−5	0	**1.77**	0.01	1.02	0.09	**0.46**	**0.09**
7	0	0	**0.60**	0.01	0.44	0.45	**0.57**	**0.45**
7	2	0	**0.68**	0.03	0.48	0.45	**0.64**	**0.45**
7	5	0	**1.66**	0.01	1.01	0.09	**0.46**	**0.09**
7	6	0	**0.71**	0.02	0.70	0.80	**0.61**	**0.80**
9	−4	0	**0.79**	0.01	0.54	0.32	**0.63**	**0.32**
9	−2	0	**0.86**	0.01	0.41	0.50	**0.77**	**0.50**
9	1	0	**0.66**	0.03	0.56	0.82	**0.53**	**0.82**
9	2	0	**0.67**	0.02	0.43	0.50	**0.77**	**0.50**
9	4	0	**0.70**	0.04	0.53	0.32	**0.63**	**0.32**

structure refinement, carried out in *Pnma*, by Dickens & Bowen (1971). The weights used for all refinements described below were $1/S^2$, where $S = [\sigma^2(F_o^2) + (0.04F_o^2)^2]^{1/2}$.

A first, full refinement was carried out in *Pnma*, excluding the 'forbidden' reflections of the data set and using anisotropic temperature factors. This resulted in a conventional R factor of 0.0186 and sensible thermal ellipsoids, but of course no calculated structure factors for the 'forbidden' reflections: it is very apparent that Bragg's comment about any distortion from the orthorhombic symmetry being very slight was totally correct. When the 'forbidden' reflections were included in a full refinement in *Pnma*, the R factor increased to 0.028.

An initial refinement in $P1$, starting with the invariant coordinates of special positions in *Pnma*, moved fractionally from these values and, when allowed to refine, yielded a Flack parameter of 0.45 (6) (Flack, 1983), a result which is indicative of inversion twinning, so further refinements were confined to the $P\overline{1}$ space group. A refinement in $P\overline{1}$, referred to later as **R1**, with anisotropic temperature factors, produced an R factor of 0.024, with sensible thermal ellipsoids (Fig. 5), but the calculated values of the structure factors for the 'forbidden' reflections were very small (of the order of 0.01), so if any are indeed present, as we believe, **there must be some structural reason other than symmetry reduction**. What could this be? The answer seems to be twinning by (pseudo-) merohedry.

This phenomenon has long been recognized. It was first noted, it seems, by Bravais, was discussed by Friedel (1926) and, more recently, by Buerger (1960), Donnay & Donnay (1974), Catti & Ferraris (1976) and Le Page *et al.* (1984), to mention the main contributors. In essence, twinning by merohedry, or 'twin-lattice symmetry', means that the individual components of the twinned crystal are related in such a way as to give rise in diffraction to an apparently regular and proper reciprocal lattice, but one whose symmetry is higher than that of the component parts – one or more of the possible twinning operations of rotation, reflection and inversion are incorporated into the diffraction symmetry of the twinned crystal, but are not symmetry elements of the individual structure.

Possible (pseudo-)merohedral twin laws were evaluated by seeking possible twofold axes (Le Page & Flack, 1995) and it was found, as expected, that all three of the aragonite cell translations are good candidates (the full orthorhombic space-group symbol is $P2_1/n2_1/m2_1/a$). There are, therefore, four possible cell orientations represented by four merohedral twinning operations. These are given below in matrix form for

real space (*hkl*) only, but are the same for reciprocal space (*xyz*).

Twin *h* =	(1.00	.00	.00)	*h*	Twin *h* =	(1.00	.00	.00)	*h*
Twin *k* =	(.00	1.00	.00)	*k*	Twin *k* =	(.00	−1.00	.00)	*k*
Twin *l* =	(.00	.00	1.00)	*l*	Twin *l* =	(.00	.00	−1.00)	*l*
Twin *h* =	(−1.00	.00	.00)	*h*	Twin *h* =	(−1.00	.00	.00)	*h*
Twin *k* =	(.00	−1.00	.00)	*k*	Twin *k* =	(.00	1.00	.00)	*k*
Twin *l* =	(.00	.00	1.00)	*l*	Twin *l* =	(.00	.00	−1.00)	*l*

The least-squares refinement program *LSLS* (Blanc & Schwarzenbach, 1995), which can incorporate these possible twinning operations and allows the refinement of the relative proportions of each twin, was used in the following refinement strategies:

(i) **R1**: Refinement in $P\bar{1}$, as mentioned above, in which twinning was not introduced. The resultant *R* factor was 0.024, but the calculated structure factors for the 'forbidden' reflections were close to zero. $\Delta\rho_{(\min,\,\max)}$, −0.72, 0.77 e Å^{-3}.

(ii) **R2**: Refinement in $P\bar{1}$ of all variable parameters, including relative twin proportions and anisotropic temperature factors. The resultant *R* factor was 0.022. However, the shapes of the derived thermal ellipsoids were not realistic (Fig. 6). The twin parameters obtained were: 0.278 (3), 0.221 (3), 0.200 (3) and 0.301 (3).

(iii) **R3**: As for **R2**, but with isotropic temperature factors. The *R* factor was 0.039.

(iv) **R4**: A $P\bar{1}$ refinement in which the anisotropic temperature factors from the first, non-twinned $P\bar{1}$ refinement (**R1**) were used and held invariant, as were the relative twin proportions from **R2** above. The resultant *R* factor was 0.025.

Table 4
Selected bond distances and angles (Å, °).

Ca1—O2	2.6572 (11)	Ca2—O61	2.4347 (10)
Ca1—O3	2.4553 (10)	Ca2—O11	2.6453 (11)
Ca1—O6	2.5496 (8)	Ca2—O51	2.5202 (9)
Ca1—O21	2.6503 (11)	Ca2—O12	2.4245 (7)
Ca1—O41	2.5013 (9)	Ca2—O42	2.5557 (9)
Ca1—O51	2.4444 (10)	Ca2—O62	2.5281 (8)
Ca1—O32	2.5592 (9)	C1—O1	1.2690 (10)
Ca1—O52	2.5433 (9)	C1—O3	1.3044 (13)
Ca1—O22	2.4074 (7)	C1—O5	1.2798 (13)
Ca2—O1	2.6638 (11)	C2—O2	1.2888 (10)
Ca2—O3	2.5086 (9)	C2—O4	1.2917 (14)
Ca2—O41	2.4524 (10)	C2—O6	1.2766 (13)
O1—C1—O3	119.00 (10)	O2—C2—O4	118.82 (10)
O1—C1—O5	121.38 (10)	O2—C2—O6	121.77 (10)
O3—C1—O5	119.40 (8)	O4—C2—O6	119.34 (8)

(v) **R5**: As for **R4**, but setting the invariant twin proportions at 0.25. The *R* factor was 0.026. $\Delta\rho_{(\min,\,\max)}$, −1.89, 2.14 e Å^{-3}. In **R5** (and **R4**) the peaks and holes in the difference map > 1 e Å^{-3} were in the range of 0.21–0.29 Å from atomic sites.

We have rejected refinement **R2**, despite it having the lowest *R* factor, owing to the physically unreal displacement ellipsoids which result from it. We also exclude refinement **R3**, but there is little to choose between **R4** and **R5**.

Our next step was to analyse the data for all the 168 'forbidden' reflections and we have done this by calculating the *R* factors (R_f) for these alone for each refinement: the results are revealing. Table 3 shows the comparison between F_{obs} and F_{calc} for each refinement, listing only those reflections with $I_{obs} > 2\sigma I_{obs}$.

For the first, non-twinned $P\bar{1}$ refinement, **R1**, R_f is 0.96 – virtually 100% – consistent with the very low values for F_{calc}.

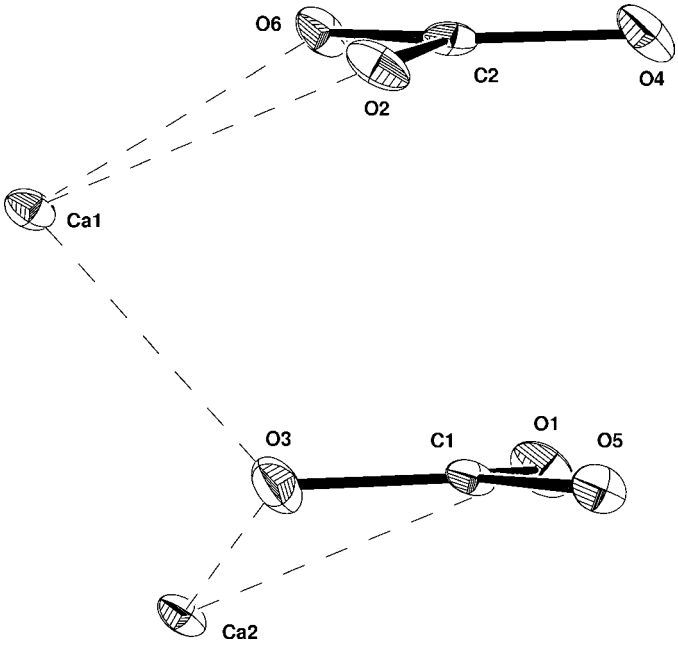

Figure 6
A view of the abnormal displacement ellipsoids obtained in refinement **R2** at the 50% probability level.

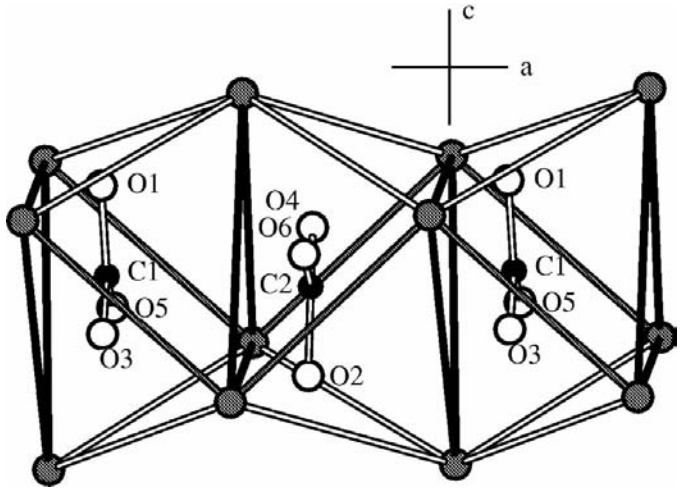

Figure 7
A single chain (...C1...C2...C1...) of face-sharing Ca_6C octahedra: C atoms in black; Ca atoms in grey; O atoms in white. Shared octahedral faces are outlined in black. The equatorial planes of the octahedra zigzag along the *a* axis and are outlined in black and grey. The two C1 atoms are one *a* lattice translation apart. The C1 atoms are slightly displaced to the left from the O1···O3···O5 plane: the C2 atom displacement from the O2···O4···O6 plane is to the right.

Table 5
Individual bond valencies, bond-valence sums (BVS) and coordination numbers (CN).

	v O1	*v* O2	*v* O3	*v* O4	*v* O5	*v* O6	**BVS**	**CN**
Ca1		0.3041 0.1578 0.1548	0.2673 0.2018	0.2359	0.2753 0.2107	0.2071	**2.015**	9
Ca2	0.2904 0.1598 0.1522		0.2313	0.2694 0.2037	0.2242	0.2824 0.2195	**2.033**	9
C1	1.3872	[0.0081] [0.0060]	1.2597	[0.0105] [0.0091]	1.3474	[0.0095] [0.0093]	**3.994**	3
C2	[0.0082] [0.0062]	1.3147	[0.0097] [0.0095]	1.3050	[0.0095] [0.0093]	1.3581	**3.978**	3
BVS	**1.990**	**1.931**	**1.960**	**2.014**	**2.058**	**2.067**		
CN	1 + 3	1 + 3	1 + 3	1 + 3	1 + 3	1 + 3		

For refinement **R2**, the R_f value is lowest at 0.56, but this has been rejected on other grounds. For refinements **R4** and **R5**, the values for R_f are 0.67 and 0.65 respectively, and again there is little to choose between them (the only difference is in the relative twin proportions). However, there is a significant difference between the twinned and untwinned situations and we conclude that **it is only the introduction of merohedral twinning which gives rise to any significant, calculated intensity for the 'forbidden' reflections**.

We now face a dilemma. On the one hand, **R2**, while having the lowest *R* factor and the flattest difference map, gives rise to displacement ellipsoids that appear unreasonable. On the other hand, **R4** and **R5**, between which we make virtually no distinction, have sensible displacement ellipsoids but difference maps which are not acceptably flat. This raises the issue of whether or not the normal criteria apply in the context of merohedral twinning.

We have chosen to use **R5** for our model of aragonite. The choice of **R5** over **R4** is based on our intuitive feeling that fine-scale twinning would give rise to equal probability for all possible orientations. The atom parameters obtained in **R5** are archived in the CIF and it is clear from these that while the *y* parameters of Ca2 and O2 do not differ significantly from the special values in *Pnma*, those for Ca1, C1, C2 and O1 are considerably and significantly different. Table 4 contains selected bond distances and angles. Table 5 gives the results of a *EUTAX* (Brese & O'Keeffe, 1991) calculation of individual bond valences and bond-valence sums. The former were calculated from the equation $v = \exp[(R - d)/0.37)]$, where R is a constant and d the measured bond length. For Ca—O bonds R is 1.967, for C—O bonds it is 1.390.

4. Crystal chemistry of aragonite

In describing the structure of aragonite, there has been much comment over the years on its relationship to the NiAs-type structure (calcite has been related in like manner to the rock-salt type). Indeed, both structures are well described as 'stuffed alloys' (O'Keeffe & Hyde, 1985). In this context, the alloy is CaC, with the *anti*-NiAs-type structure: the O atoms of the carbonate group constitute the 'stuffing'. One description has C atoms occupying octahedral sites in a hexagonal close-packed array of Ca atoms and these CCa_6 octahedra form columns along [100] by face-sharing (Fig. 7): adjacent octahedral columns share edges. An alternative, but equally valid, description has Ca atoms coordinated by six C atoms at the vertices of a trigonal prism and these share edges to fill space. However, the presence of O atoms in the carbonate groups leads to considerable distortion of these polyhedra: the equatorial planes of the octahedra have become more rectangular as a consequence of the non-bonded O—O repulsion, as have the 'square' faces of the trigonal prisms. In this context, the ideas of O'Keeffe & Hyde (1976, 1978*a*,*b*, 1982) are particularly germane.

The various attractive and repulsive interactions are complex and result in the carbonate ion being off-centre in the CCa_6 octahedra, as can be seen from Fig. 7. Moreover, all four independent refinements of this structure, cited previously, where the symmetry was assumed to be *Pnma*, and especially the neutron diffraction study by Jarosch & Heger (1986), had found that the CO_3 ion is not planar; the C atom being $\sim$0.025 Å out of the plane of its three strongly coordinated O atoms. Our results confirm this for both C atoms in the $P\overline{1}$ refinements. C1 is 0.035 (1) Å from the plane of O1, O3 and O5, and C2 is 0.020 (1) Å from the plane of O2, O4 and O6 for **R5**. Also, more recently, Winkler *et al.* (2000) have reported a theoretical investigation of the aplanarity of carbonate groups in dolomite, aragonite and norsethite: they concluded aplanarity is indeed a property of the ground state, although in the case of aragonite, their quantum-mechanical calculations assumed the orthorhombic space group.

5. Summary and conclusions

The aragonite crystal studied clearly gives rise in diffraction to genuine Bragg reflections which are forbidden in the *Pnma* space group and significant structure factors for these are calculated in a $P\overline{1}$ refinement only if merohedral twinning is introduced. Whether or not these results can be generalized is an open question, although the neutron diffraction data on a different crystal suggest that this might be so. What is still unclear is the structural role played by lattice impurities such as Sr, which are normally present in varying amounts in natural crystals, and why it is that biogenic deposition of calcium carbonate seems to yield predominantly the metastable aragonite form.

We acknowledge with gratitude the assistance of Dr Colin Kennard, of the Queensland University Chemistry Department, who made available to us his CAD-4 diffractometer for collection of the data set used finally. Also, we acknowledge the help given by the late Dr Lindsay Davis in collection of the neutron diffraction data at ANSTO, Dr Andrew Johnson of the Electron Microscopy Centre in the University of Western Australia for the convergent-beam electron diffraction work and Dr Victor Streltsov from the same university in the later stages of the refinement.

References

Adler, H. H. & Kerr, P. F. (1963). *Am. Mineral.* **48**, 839–853.
Arndt, U. W. & Willis, B. T. M. (1966). *Single-Crystal Diffractometry*. Cambridge University Press.
Belda, C., Cuff, C. & Yellowlees, D. (1993). *J. Marine Biol.* **117**, 251–257.
Blanc, E. & Schwarzenbach, D. (1995). *LSLS Xtal*3.4 *User's Manual*, edited by S. R. Hall, G. S. D. King & J. M. Stewart. University of Western Australia, Lamb, Perth.
Bragg, W. L. (1924). *Proc. R. Soc. London A*, **105**, 16–39.
Brese, N. E. & O'Keeffe, M. (1991). *Acta Cryst.* B**47**, 192–197.
Broeker, W. S. & Oversby, V. M. (1971). *Chemical Equilibria in the Earth*. New York: McGraw Hill.
Buerger, M. J. (1960). *Crystal Structure Analysis.* New York: John Wiley.
Catti, M. & Ferraris, G. (1976). *Acta Cryst.* A**32**, 163–165.
Catti, M., Pavese, A. & Price, G. D. (1993). *Phys. Chem. Miner.* **19**, 472–479.
Cuff, C. (1969). PhD Thesis. University of London.
Dal Negro, A. & Ungaretti, L. (1971). *Am. Mineral.* **56**, 768–772.
Dickens, B. & Bowen, J. S. (1971). *J. Res. Natl. Bureau Standards A*, **75**, 27–32.
Donnay, G. & Donnay, J. D. H. (1974). *Can. Mineral.* **12**, 422–425.
Flack, H. D. (1983). *Acta Cryst.* A**39**, 876–881.
Frech, R., Wang, E. C. & Bates, J. B. (1980). *Spectrochim. Acta A*, **36**, 915–919.
Friedel, G. (1926). *Leçons de Cristallographie.* Paris: Berger-Levraut.
Gillet, G., Bullman, C., Reynard, B. & McMillan, P. (1993). *Phys. Chem. Miner.* **20**, 1–18.
Hall, S. R., King, G. S. D. & Stewart, J. M. (1995). Editors. *Xtal*3.4 *User's Manual.* University of Western Australia, Lamb, Perth.
Jarosch, D. & Heger, G. (1986). *Tschermaks Mineral. Petrogr. Mitt.* **35**, 127–131.
Kraft, S., Knittle, E. & Williams, Q. (1991). *Geophys. Res.* **96**, 17997–18009.
Le Page, Y., Donnay, J. D. H. & Donnay, G. (1984). *Acta Cryst.* A**40**, 679–684.
Le Page, Y. & Flack, H. D. (1995). *CREDUC Xtal*3.4 *User's Manual*, edited by S. R. Hall, G. S. D. King & J. M. Stewart. University of Western Australia, Lamb, Perth.
Mitscherlich, E. (1822). *ÜBer die Körper, welche in zwei verschiedene Formen krystallisieren.* Abhandlungen der Preussischen Akadamie der Wissenschaften.
Mylrea, D. K. (1991). Thesis. James Cook University, Townsville, Queensland, Australia.
O'Keeffe, M. & Hyde, B. G. (1976). *Acta Cryst.* B**32**, 2923–2926.
O'Keeffe, M. & Hyde, B. G. (1978*a*). *Acta Cryst.* B**34**, 27–32.
O'Keeffe, M. & Hyde, B. G. (1978*b*). *Acta Cryst.* B**34**, 3519–3528.
O'Keeffe, M. & Hyde, B. G. (1982). *J. Solid State Chem.* **44**, 24–31.
O'Keeffe, M. & Hyde, B. G. (1985). *Struct. Bonding*, **61**, 77–144.
Phillips, Sir D. (1979). *Biographical Memoirs of Fellows of the Royal Society*, Vol. 25, pp. 75–143. London: The Society.
Rasmussen, C. E., Cuff, C. & Hopley, D. (1992). *Proc. of the 7th Int. Coral Reef Symp.*, edited by R. H. Richmond. Guam, Micronesia.
Renninger, M. (1937). *Z. Phys.* **106**, 141–176.
Rossmanith, E. (1992). *Acta Cryst.* A**48**, 596–610.
Rossmanith, E. (1999). *J. Appl. Cryst.* **32**, 355–361.
Rossmanith, E. & Armbruster, T. (1995). *Z. Kristallogr.* **210**, 645–649.
Scheetz, B. E. & White, W. B. (1970). *Am. Mineral.* **62**, 36–50.
Villiers, J. P. R. de (1971). *Am. Mineral.* **56**, 758–767.
White, W. B. (1974). *The Infra red Spectra of Minerals*, edited by V. C. Farmer, pp. 87–110. Mineralogical Society, London.
Winkler, B., Zeman, J. & Milman, V. (2000). *Acta Cryst.* B**56**, 648–653.
Wollaston, W. H. (1812). *Dictionary of Scientific Biography*, edited by C. C. Gillispie, pp. 486–494. New York: Charles Scribner's Sons.